JOURNAL OF GEOPHYSICAL RESEARCH, VOL. 111, E09013, doi:10.1029/2006JE002706, 2006

Thermal conductivity measurements of particulate materials: 3. Natural samples and mixtures of particle sizes

Marsha A. Presley[1] and Robert A. Craddock[2]

Received 2 March 2006; revised 29 May 2006; accepted 14 June 2006; published 23 September 2006.

[1] A line-heat source apparatus was used to measure thermal conductivities of natural fluvial and eolian particulate sediments under low pressures of a carbon dioxide atmosphere. These measurements were compared to a previous compilation of the dependence of thermal conductivity on particle size to determine a thermal conductivity-derived particle size for each sample. Actual particle-size distributions were determined via physical separation through brass sieves. Comparison of the two analyses indicates that the thermal conductivity reflects the larger particles within the samples. In each sample at least 85–95% of the particles by weight are smaller than or equal to the thermal conductivity-derived particle size. At atmospheric pressures less than about 2–3 torr, samples that contain a large amount of small particles ($\leq$125 μm or 4 Φ) exhibit lower thermal conductivities relative to those for the larger particles within the sample. Nonetheless, 90% of the sample by weight still consists of particles that are smaller than or equal to this lower thermal conductivity-derived particle size. These results allow further refinement in the interpretation of geomorphologic processes acting on the Martian surface. High-energy fluvial environments should produce poorer-sorted and coarser-grained deposits than lower energy eolian environments. Hence these results will provide additional information that may help identify coarser-grained fluvial deposits and may help differentiate whether channel dunes are original fluvial sediments that are at most reworked by wind or whether they represent a later overprint of sediment with a separate origin.

Citation: Presley, M. A., and R. A. Craddock (2006), Thermal conductivity measurements of particulate materials: 3. Natural samples and mixtures of particle sizes, *J. Geophys. Res.*, *111*, E09013, doi:10.1029/2006JE002706.

1. Introduction

[2] Previous experiments [*Presley and Christensen*, 1997b] (hereinafter referred to as Paper 2) have demonstrated that the thermal conductivity of particulate materials is related to the particle size and the atmospheric pressure of carbon dioxide over a wide range of atmospheric pressures (1–100 torr; 1 torr = 1.33 mbar = 1.316×10^{-3} atm = 133.3 Pa). This relationship is illustrated in Figure 1 for an atmospheric pressure of 5 torr and can be approximated by the empirical equation

$$\kappa = (C \cdot P^{0.6}) d^{-0.11 \cdot \log(P/K)} \quad (1)$$

where κ is the thermal conductivity in W m^{-1}K^{-1}, P is atmospheric pressure in torr, d is the particle diameter in μm, and C and K are constants. When these units are used, $C \approx 0.0015$ and $K \approx 8.1 \times 10^4$.

[3] The particle size of surficial units on Mars can be estimated by using equation (1) together with thermal inertia derived from brightness temperature observations by either the Mars Odyssey Thermal Emission Imaging Spectrometer (THEMIS) [*Fergason and Christensen*, 2003; *Putzig et al.*, 2004; *Fergason et al.*, 2006b], the Mars Global Surveyor Thermal Emission Spectrometer (TES) [*Mellon et al.*, 2000; *Putzig et al.*, 2005], the Viking Infrared Thermal Mapper [*Kieffer et al.*, 1977; *Christensen and Malin*, 1988; *Haberle and Jakosky*, 1991], the Mariner 9 Infrared Radiometer [*Kieffer et al.*, 1973], or the miniTES aboard the both of the Mars Exploration Rovers (MER), Spirit and Opportunity [*Fergason et al.*, 2006a]. These particle size estimates can then be used to characterize surficial units in terms of their depositional history and origin [e.g., *Kieffer et al.*, 1981; *Presley and Arvidson*, 1988; *Edgett and Christensen*, 1991; *Christensen and Moore*, 1992; *Merényi et al.*, 1996; *Mellon et al.*, 2000; *Putzig et al.*, 2005; *Fergason et al.*, 2006b].

[4] The data used to derive equation (1), however, were obtained from glass beads sorted into very narrow particle size ranges [*Presley*, 1995]. What can equation (1) tell us then about *real* surficial deposits, in which the particles can be angular or platy as well as rounded, and which may contain a wide range of particle sizes? This question is addressed by measuring the thermal conductivities of sev-

[1] School of Earth and Space Exploration, Mars Space Flight Facility, Arizona State University, Tempe, Arizona, USA.
[2] Center for Earth and Planetary Studies, National Air and Space Museum, Smithsonian Institution, Washington, D. C., USA.

0148-0227/06/2006JE002706$09.00

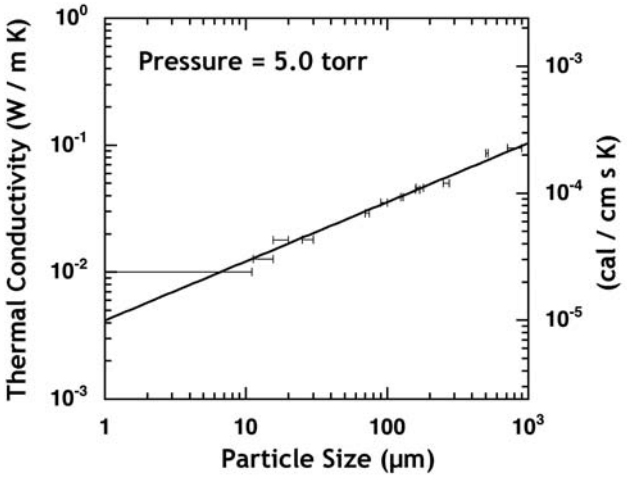

Figure 1. Thermal conductivity plotted against particle size for an atmospheric pressure of 5.0 torr (Mars datum is set at 4.6 torr or 6.1 mbar). This figure is from Figure 8f of Paper 2.

eral natural samples, collected from both eolian and fluvial environments, and a simulated Martian sediment (a.k.a. JSC Mars-1 [*Allen et al.*, 1998]), under low atmospheric pressures applicable to the Martian surface.

[5] This paper begins with a brief review of the factors that can affect the thermal conductivity of particulate materials, particularly under Martian atmospheric pressures. Section 3 provides a description of the experimental set-up and procedure. Section 4 is a presentation of the data collected, while section 5 is a report of the results. A discussion follows in section 6, and conclusions are presented in section 7.

2. Thermal Conductivity Review

[6] The bulk thermal conductivity of a particulate material is composed of additive contributions from three primary heat transfer mechanisms: (1) conduction by the gas present in the void space between the particles, κ_g; (2) conduction within the solid particles and across interparticle contacts, κ_s; and (3) thermal radiation within the particles, across the void spaces between particle surfaces, and between void spaces, κ_r:

$$\kappa = \kappa_{eff} = \kappa_g + \kappa_s + \kappa_r \tag{2}$$

Particle-particle contacts behave like thermal capacitors, in the sense that heat builds up around the contacts, and hence significantly reduce the contribution from κ_s. The composition of the particles does not significantly affect the bulk thermal conductivity, then, since $\kappa_g \gg \kappa_s$ [*Wechsler et al.*, 1972]. *Smoluchowski* [1910] and *Watson* [1964] demonstrated experimentally, however, that even under a vacuum, where κ_g becomes zero, the composition of the particles is still not a significant factor.

[7] The contribution from radiation, κ_r, is proportional to T^3, where T is temperature [*Watson*, 1964], and for high temperatures radiation becomes an increasingly significant factor. For temperatures less than 300 K, however, $\kappa_g \gg \kappa_r$ for most particulate materials, even at atmospheric pressures as low as 1 torr. *Schotte* [1960] relates that the radiative contribution becomes significant for 1 mm particles only above 400°C, and for 100 μm particles only above 1500°C, and that these limits will hold for nonspherical as well as spherical particles. *Fountain and West* [1970] measured thermal conductivities of dry, particulate basalt over a range of temperatures, 207° to 318°C, and observed only a very slight increase in thermal conductivity over this range.

[8] The conductivity of a gas has been shown to be equal to [e.g., *Kennard*, 1938]

$$\kappa_g = A\eta c_V \tag{3}$$

where A is a coefficient that depends on the composition of the gas (1.64 for CO_2 and 1.91 for N_2), c_V is the specific heat at constant volume, and η is the shear viscosity, which in turn equals [e.g., *Kennard*, 1938]

$$\eta = 0.499\rho\overline{\nu}L = \frac{5\pi(mkT/\pi)^{1/2}}{16\pi\sigma^2} \tag{4}$$

where ρ is the density of the gas, $\overline{\nu}$ is the mean molecular velocity and L is the mean free path or average distance between molecular collisions, m is the molecular mass, k is Boltzmann's constant, T is temperature, and σ is the effective molecular diameter (0.46 nm for CO_2 and 0.32 nm for N_2) [e.g., *Moore*, 1972].

[9] Under Martian environmental conditions, the thermal conductivity of the atmospheric gas is the primary determinant of the bulk thermal conductivity, which in turn depends on the mean free path within the gas. The mean free path of the gas molecules depends on both the pressure of the gas and its temperature. Martian atmospheric pressures range from <1 torr at the top of Olympus Mons to 7 torr at the bottom of Hellas Basin, and Martian surface temperatures range from a low of 148 K at the poles to a high of 315 K at midday during the summer in mid-southern latitudes [*Carr*, 1981; *Kieffer et al.*, 1992; J. Bandfield, personal communication, 2006]. As illustrated in Table 1, the mean free path of carbon dioxide gas molecules should range from 2–35 μm under Martian atmospheric conditions, which is approximately the same order of magnitude as the effective distance over which conduction takes place between the particles (Note: this table is a both a correction and an update to that published by *Presley and Christensen* [1997c]).

[10] Conduction primarily occurs near the points of contact between the particles [*Deissler and Boegli*, 1958], and the effective conduction distance is approximately one-sixth the particle diameter or less [*Woodside and Messmer*, 1961]. Gas molecules are thus as likely to

Table 1. Mean Free Path of Carbon Dioxide Under Extremes of Martian Surface Conditions[a]

	Temperature	
Pressure, torr	148 K	315 K
1	16 μm	35 μm
7	2.3 μm	5.0 μm

[a]Assumes a molecular diameter of 0.46 nm [*Moore*, 1972].

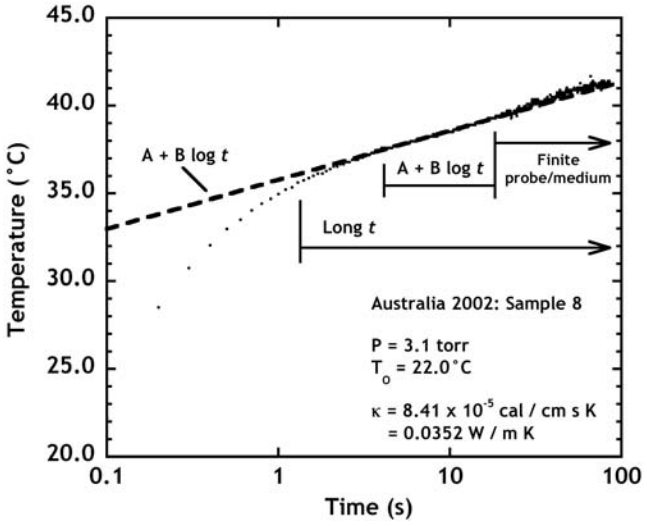

Figure 2. Illustration of the different time regimes in a plot of the change in temperature (T) versus log time elapsed (t). Effects from either the sample boundaries or axial heat loss may cause an extra rise in T, as it typically does for this experimental setup, or a drop in T [cf. *Jones*, 1988].

collide with the solid particles as they are with each other, and the average heat transfer distance between particles, which is related to pore size and shape, will determine how fast heat will flow through a particulate material [*Schotte*, 1960]. Particle shape, bulk density of the material, and particle size will affect the average heat transfer distance between particles and therefore the thermal conductivity of the material. The effect of particle size, within narrow ranges, was addressed in Paper 2 of this article series. This paper will address the effects on thermal conductivity of a mixture of particle sizes, particularly the range that is found in natural eolian and fluvial deposits. Bulk density and particle shape will be addressed in Papers 4 and 5 of this series (study in progress).

3. Experimental Method

3.1. Experimental Apparatus

[11] The line-heat source method was chosen for this project due to its relative simplicity and proven reliability [*Cremers*, 1971; *Presley and Christensen*, 1997a] (the latter is hereinafter referred to as Paper 1). The experimental apparatus was described in detail in Paper 2.

3.1.1. Electronics Upgrades

[12] The thermocouple and heating wire were connected to a National Instruments PCI-1200 analog to digital (A/D) circuit board, which replaced the Lab-SE A/D board. This increased the voltage resolution from 8-bit to 12-bit. The signal conditioner described in Paper 1, which amplifies and offsets the voltage signals to take advantage of the full 10 V range of the A/D board was adjusted to accommodate the new resolution. The computer used to process the resulting data was upgraded from the Mac SE to a Mac G4 Tower.

3.1.2. Vacuum Equipment

[13] When approximately 70% of the thermal conductivity measurements for this study had been completed, the Sargent Welch 1400 duo-seal vacuum pump began to leak oil and was replaced for the remainder of the project with a Sargent Welch 8815 DirecTorr vacuum pump, with a Sargent Welch 1417A Filter over the exhaust port to remove oil fumes.

3.1.3. Sample Holder

[14] While all other equipment remains as described in Paper 1, a brief description of the sample holder bears repeating. The sample holder design was copied from that of *Cremers* [1971] and fabricated from Teflon. A rectangular hole, 50 mm × 25 mm, with a 25 mm depth, was fashioned in the Teflon to hold the sample. A 0.003-inch (0.075 mm; 40 AWG) platinum wire is strung across the middle of the cavity and spring-loaded on one end to minimize movement of the wire within the sample when the wire expands with applied heat. The platinum wire has the dual purpose of acting as a heat source with the application of a constant current, and as a thermometer. The change in resistivity of the platinum wire over the course of a run is related to the temperature of the sample in contact with it [*McGee*, 1988]. Two leads of the same gauge platinum are spot welded to either end of the heating wire in order to measure that change in resistivity.

3.2. Experimental Procedure

[15] The sample holder is placed inside a vacuum chamber. The sample is baked for 24 hours at ~100°C to drive off condensed volatiles. The ambient atmosphere is then evacuated from the chamber, while the sample is baked for an additional 24 hours. The system is then allowed to cool to room temperature (~24°C), and the chamber is back filled with carbon dioxide to the desired atmospheric pressure. The system is capable of reaching and maintaining atmospheric pressures from 0.01 to 100 torr.

[16] The line-heat method is based on the assumption of radial diffusion of heat from a line-heat source [*Stalhane and Pyk*, 1931; *Carslaw and Jaeger*, 1959]:

$$\frac{\partial T}{\partial r} = \frac{\alpha}{r}\frac{\partial}{\partial r}\left(r\frac{\partial T}{\partial r}\right) \tag{5}$$

where $\alpha(=\kappa/\rho c)$ is the thermal diffusivity of the sample, κ is its thermal conductivity, ρ is its bulk density, and c is its specific heat; T is temperature; t is time; and r is the radial distance from the heat source. With appropriate boundary

Table 2. Bulk Densities of the Samples in Situ, Before Collection, and as Placed in the Sample Holder

	Density, kg/m^3	
Sample	In Situ	In Sample Holder
1	1600	1600
2	1500	1450
3	1500	1650
4	1500	1600
5	1500	1600
6	1500	1400
7	1500	1400
8	1300	1200
JSC-1	N/A	1300

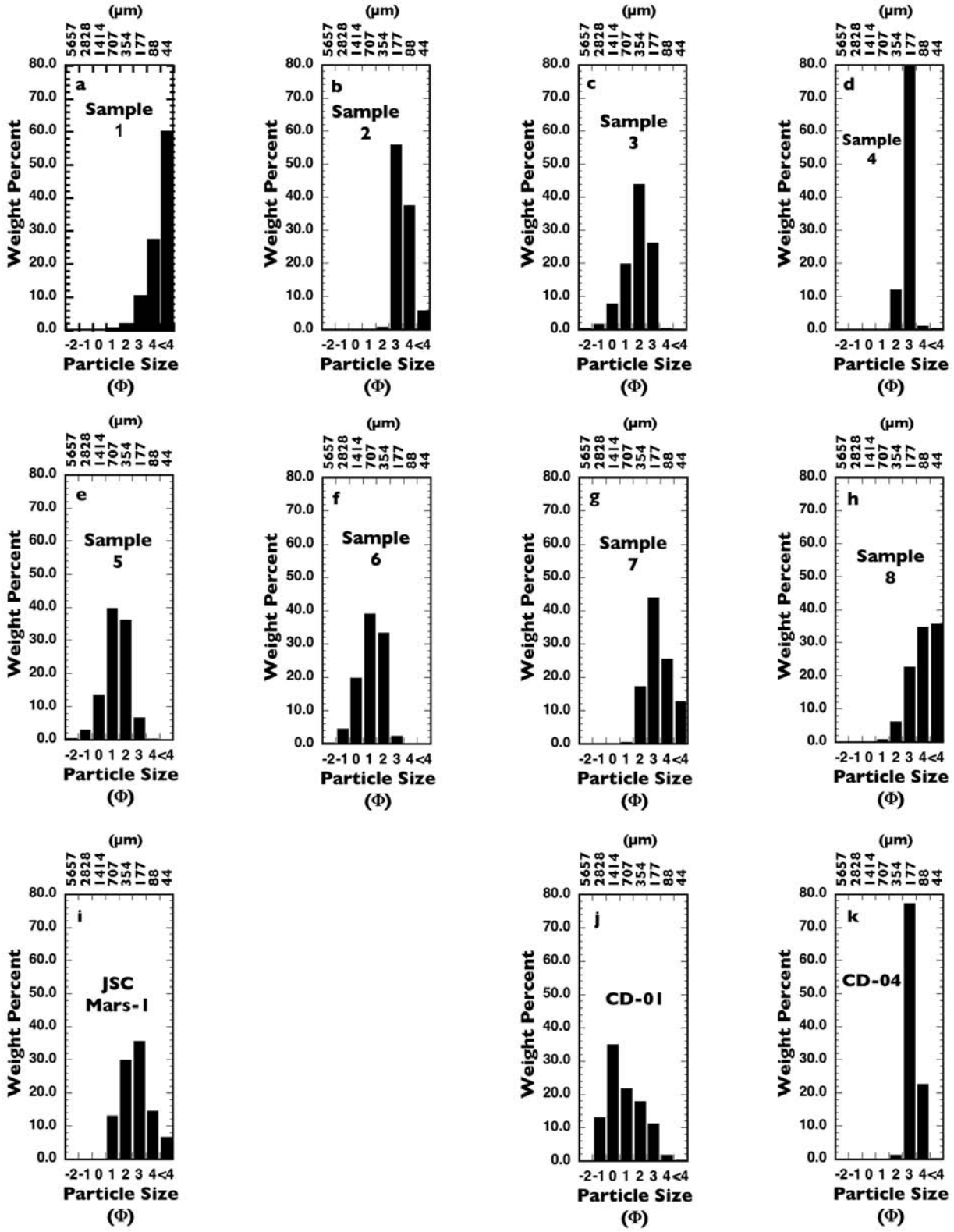

Figure 3. Particle sizes of the samples investigated in bins of Φ, where $\Phi = -\log d$, and plotted as histograms. (a–h) Samples 1–8 were collected from various fluvial and eolian environments in the Simpson Desert, Australia. (i) JSC Mars-1 is a simulated Martian regolith [*Allen et al.*, 1998]. Samples (j) CD-01 and (k) CD-04 are dune sands from the San Francisco volcanic fields and are included here for comparison purposes (results originally published by *Presley and Christensen* [1997c]).

Table 3. Statistical Parameters of the Particle Size Distribution of the Samples

	Median Particle Size		Mean Particle Size		Sorting		Skewness	
Sample	Φ	μm	Φ	μm	Value	Description	Value	Description
A-1[a]	4.18	55	4.01	62	0.81	moderately sorted	−0.38	strongly coarse skewed
A-2	2.89	135	2.94	130	0.61	moderately well sorted	0.16	fine skewed
A-3	1.50	354	1.42	374	0.93	moderately sorted	−0.19	coarse skewed
A-4	2.45	183	2.44	184	0.34	very well sorted	−0.06	nearly symmetrical
A-5	0.88	543	0.82	566	0.87	moderately sorted	−0.12	coarse skewed
A-6	0.68	624	0.63	646	0.90	moderately sorted	−0.12	coarse skewed
A-7	2.72	152	2.83	141	0.93	moderately sorted	0.20	fine skewed
A-8[a]	3.60	82	3.55	85	0.98	moderately sorted	−0.13	coarse skewed
JSC Mars-1	2.19	219	2.22	215	1.14	poorly sorted	0.05	nearly symmetrical
CD-01	0.10	933	0.33	796	1.24	poorly sorted	0.28	fine skewed
CD-04	2.75	149	2.75	149	0.36	very well sorted	0.06	nearly symmetrical

[a]A significant amount of Sample 1 and Sample 8 may belong in 5 Φ or smaller. As such, the statistical parameters may be skewed for these two samples.

conditions, the solution for this equation can be expressed as [*Carslaw and Jaeger*, 1959]

$$T_2 - T_1 = \frac{q}{4\pi\kappa} \ln\frac{t_2}{t_1} \tag{6}$$

where q is the power applied to the heating wire. Thus, when heat is applied to a sample from a line-heat source, the thermal conductivity is determined by plotting the temperature of the sample against the log of time elapsed, and applying equation (6) to the linear portion of the long-time domain (Figure 2) [cf. *Jones*, 1988, Figure 2]:

$$\kappa = \frac{q(\ln 10)}{4\pi m} \tag{7}$$

where m is the slope of the linear portion of the curve. The factor of ln 10 is included to convert from the natural log scale to a log (10) scale.

[17] A constant current is applied to the heating wire for a time, $\Delta t = 90$ s. The limitations of the length of time (Δt) per run, based on the wire and sample dimensions, were discussed in Paper 1. Calculations indicate that, for this experimental setup and expected thermal conductivities, a 90 s run time is sufficient to reach the very long time regime assumed in the derivation of equation (4), without significant error from either axial heat loss or sample boundary effects.

[18] The voltage across the heating wire as a result of the applied current is recorded every 0.1 s with the A/D board and signal conditioner previously mentioned and specifically developed software [*Presley*, 1995]. These voltages are converted into resistances by dividing by the constant current applied during the run. The resistances are then translated into temperatures following the relationship of platinum resistance to temperature provided by *McGee* [1988] (see also Paper 2 for more detail).

[19] The temperature values are plotted versus log time elapsed. The slope, m, of the straight-line portion in the long-time domain (Figure 2) is determined through a linear regression curve fitting routine:

$$m = \frac{\Delta T}{\Delta(\log t)} = \frac{T_2 - T_1}{\log\left(\frac{t_2}{t_1}\right)} \tag{8}$$

The thermal conductivity is then computed from equation (7). The power q is calculated as the average of the voltages recorded over the length of the run multiplied by the value of the current applied. The deviation from the assumption of constant power, rather than constant current, is relatively minor and addressed in the error analysis section of Paper 2.

3.3. Samples

[20] Eight samples were collected from various eolian and fluvial environments in the Simpson Desert, Australia. For a brief overview of the field sites and geological context, see *Craddock and Presley* [2003]. At each site, two small cores, approximately 8 cm in-depth with a 2.5 cm radius, were obtained in close proximity (~20 cm apart) with a brass collection tube tightly capped at each end immediately after collection. One core was used for particle size analysis and the other was used for the thermal conductivity measurements. The bulk density and moisture content of the surface material immediately adjacent to both samples were measured in situ prior to extraction of the samples with a Model 3440 portable surface moisture density gauge manufactured by Troxler Electronic Laboratories. The moisture content assured us that we were collecting dry samples (i.e., that it had not rained recently). The density measurements assured that the appropriate bulk density was applied in the laboratory, as thermal conductivity will vary with bulk density [*Fountain and West*, 1970; *Presley and Christensen*, 2006].

[21] Each sample was poured into the cavity of the sample holder from a height typically less than 1 cm above the cavity, as previously described (Paper 2). The top of each sample is carefully leveled so that the volume of the sample can be equated to that of the cavity. This action may increase the packing very slightly at the top of the sample, but will not affect the value of either the overall bulk density, or the packing of the sample in the vicinity of the heating wire, 1.75 cm below the surface of the sample. The bulk densities of the sample prepared this way were within 100 kg/m^3 of their bulk densities in situ (Table 2).

[22] Particle size distribution was determined by physically separating the particles through brass sieves corresponding to Φ size intervals ($\Phi = -\log_2 d$, where d is the particle diameter in millimeters). Particle size

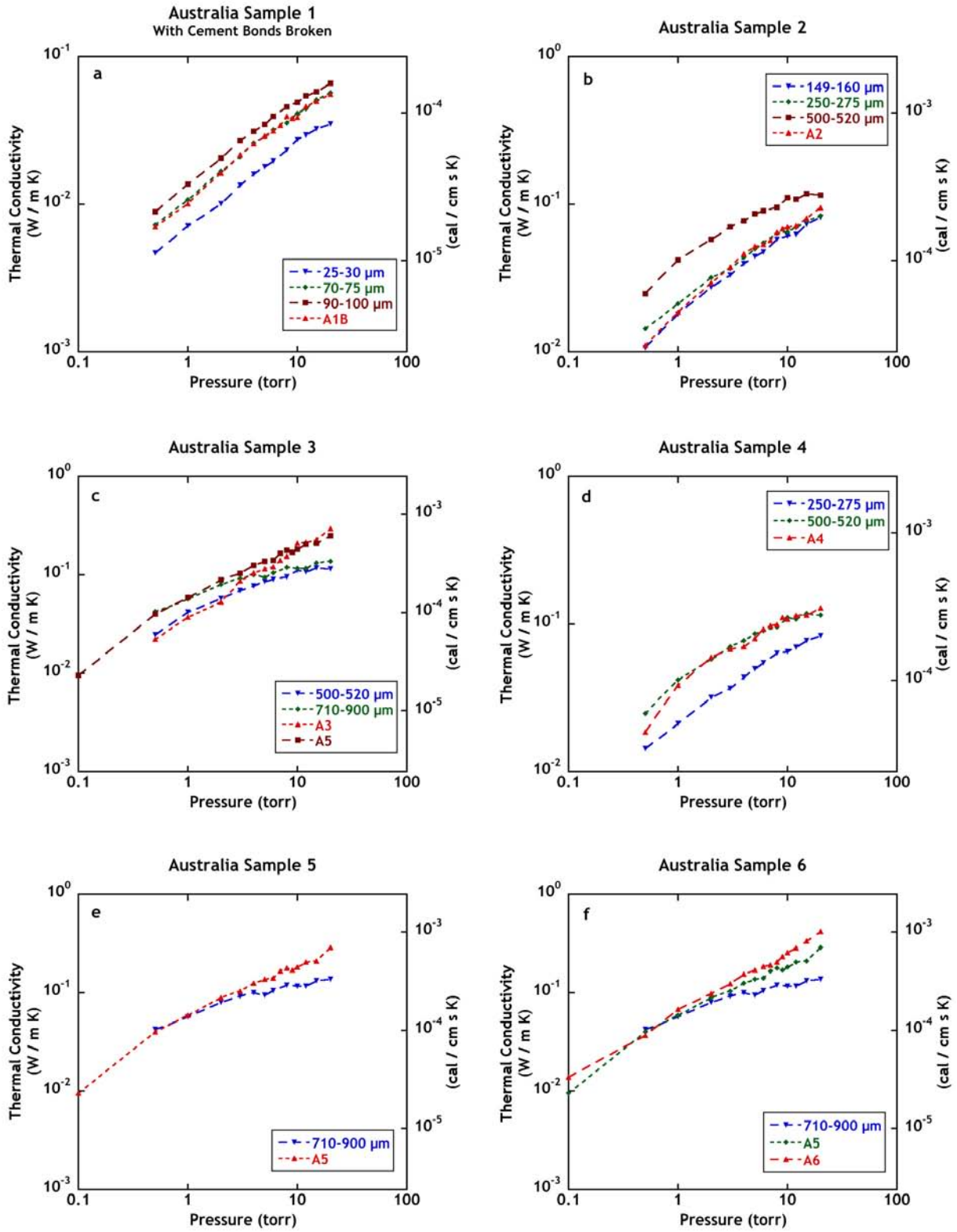

Figure 4. Plots of thermal conductivity versus atmospheric pressure for each of the eight Australian samples, the Mars simulant, and basaltic dune sands, CD-01 and CD-04. Included in each plot are thermal conductivity data for glass beads (Paper 2) of appropriate particle size for comparison. Thermal conductivities are presented here in SI units (W m^{-1} K^{-1}) on the primary *y* axis and in cgs units (cal cm^{-1} s^{-1} K^{-1}) on the secondary *y* axis. (a) Sample 1, (b) Sample 2, (c) Sample 3, (d) Sample 4, (e) Sample 5, (f) Sample 6, (g) Sample 7, (h) Sample 8, (i) simulated Martian regolith, JSC Mars-1, (j) coarse basaltic dune sand, CD-01, and (k) fine basaltic dune sand, CD-04.

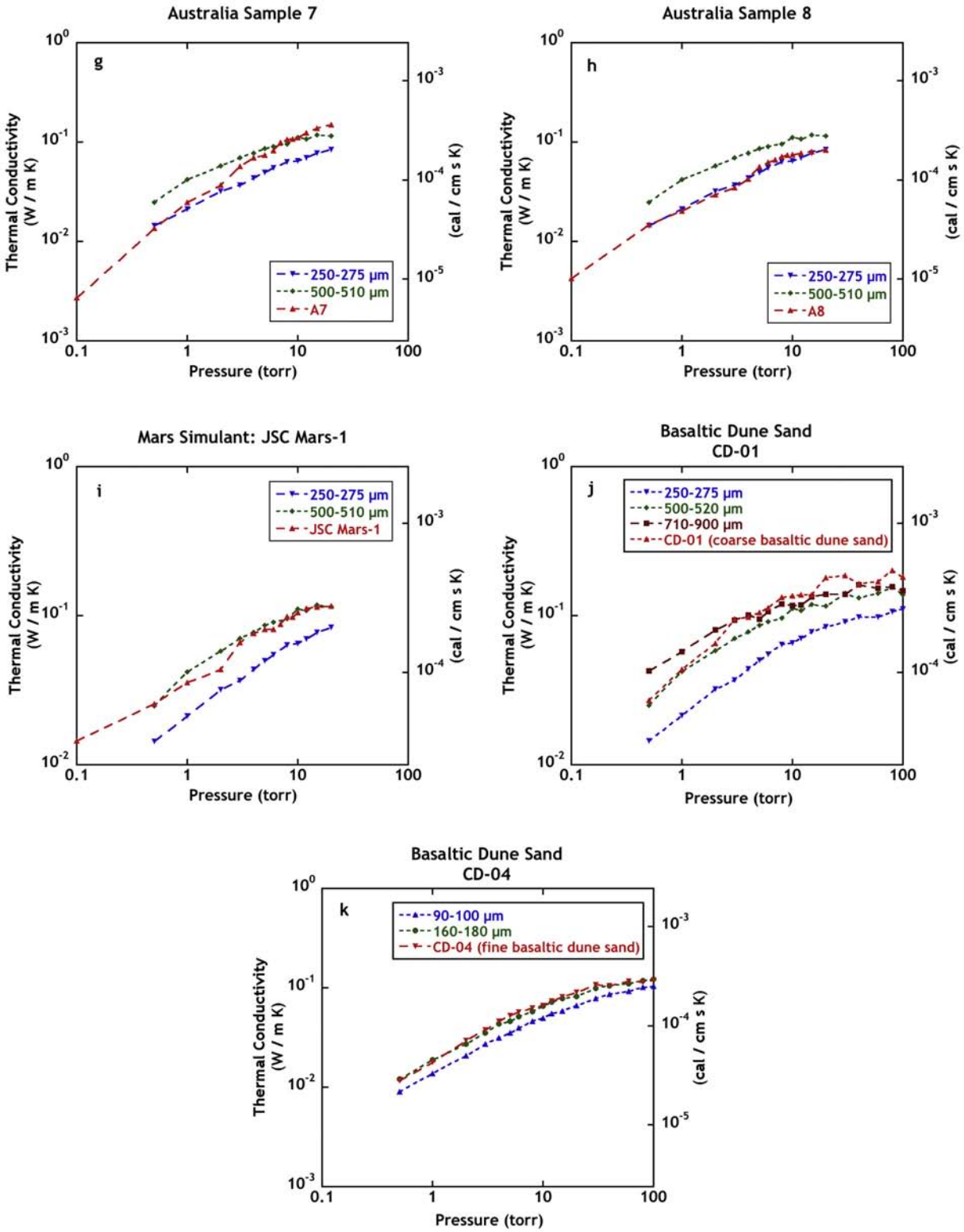

Figure 4. (continued)

distributions by weight percent for each sample are displayed as histograms in Figure 3, both in Φ and in μm, and the statistics describing the particle size distribution are summarized in Table 3. Two samples from a previous analysis [*Presley and Christensen*, 1997c], CD-01 and CD-04, are included in Figures 3 and 4 and in the analysis in sections 5 and 6, for comparison. These samples, coarse (CD-01) and very fine (CD-04) basaltic dune sand, were collected from the San Francisco Volcanic Field and characterized by A. H. Levine (unpublished manuscript,

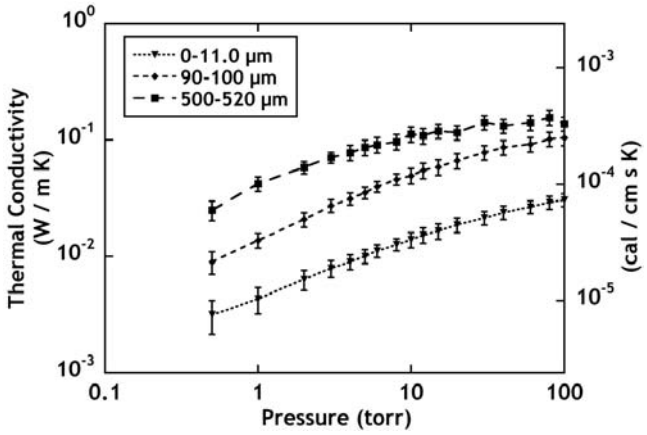

Figure 5. Instrumental error. This figure is a plot of thermal conductivity versus atmospheric pressure for <11 μm, 90–100 μm, and 500–520 μm glass beads. The error bars represent the maximum instrumental error for the measurements. This figure is from Figure 9 in Paper 2.

1990). Particles in all of the samples were relatively well rounded.

4. Data

4.1. Measurements

[23] Temperature versus elapsed time measurements were obtained for each of the eight samples and the JSC Mars-1 simulant for several pressures ranging from 0.1 torr to 20 torr. This range of pressures extends beyond those expected on the Martian surface (1–7 torr) so that a sufficiently large curve would be available for comparison to previous work (0.01–100 torr) on the effect of particle size on thermal conductivity (Paper 2). Figure 4 presents a summary plot for each sample, with thermal conductivity plotted versus atmospheric pressure. Each plot includes curves for glass beads of comparable particle size ranges, previously presented in Paper 2 and by *Presley* [1995]. Also included are plots for basaltic dune sand samples, CD-01 and CD-04, data for which were previously presented by *Presley and Christensen* [1997c].

4.2. Precision and Accuracy

[24] A detailed error analysis of the experimental technique is presented in Paper 2. In summary, maximum instrumental errors of 10–15% were calculated for thermal conductivities between 0.008 and 0.1 $W/m^{-1}K^{-1}$, and maximum instrumental errors of 15–30% for thermal conductivities beyond this range. These calculated errors were verified by examining both the reproducibility of the measurements and their internal consistency (Paper 2). The typical precision of the measurements is ±5% for thermal conductivities between 0.008—0.1 $W/m^{-1}K^{-1}$. For thermal conductivities outside of this range, the precision errors reach ±15%. Figure 5 illustrates the maximum instrumental errors calculated for samples of glass beads with diameters <11 μm, 90–100 μm, and 500–520 μm (originally presented in Paper 2). The electronics upgrades did not significantly affect assessment of instrumental precision, as these upgrades were made primarily to improve the ease in data collection and precision improvements were minor.

[25] The lack of a low thermal conductivity standard continues to prohibit a true assessment of the accuracy of these measurements. The most accurate thermal data available for the atmospheric pressure range considered here are those from *Wechsler and Glaser* [1965] and *Smoluchowski* [1910]. Their data are compared in Paper 2 to the thermal conductivities previously measured with this laboratory set-up. That comparison indicated that the thermal conductivities from this lab matched those from these other investigators within the error of precision.

[26] More recently, estimations of thermal conductivities were obtained from a "Mars Microprobe-type penetrator" in preparation for the DS-2 Mars Microprobe mission [*Smrekar et al.*, 1999; *Urquhart and Smrekar*, 2000]. These data, collected and processed by Mary Urquhart and Susan Smrekar, were never published, in part due to the failure of the mission, but are presented in Table 4. Their data match data from this laboratory for the appropriate particle sizes within 3% in 4 of the 6 measurements, and within 30% for all six measurements.

[27] In addition, *Fergason et al.* [2006a] applied the relationship of particle size and thermal conductivity (Paper 2) to thermal inertias computed for several areas examined by the Mars Exploration Rovers. The derived particle sizes were generally consistent with particle sizes measured by the Microscopic Imagers (MI) aboard each Rover.

5. Results

[28] The largest particle sizes previously investigated were 710–900 μm (Paper 2). Figure 4 illustrates that four of the eleven samples (Samples 3, 5, 6 & CD-01) manifested considerably higher thermal conductivities than those measured for the 710–900 μm glass beads. These results are consistent with the presence of material larger than 710–900 μm (1 Φ) in each of these samples, as illustrated in Figures 3c, 3e, 3f, and 3j. Glass beads or other material larger than 1 mm that would be required to make suitable particle size "standards" currently are not available in sufficient quantities. Thus, in order to evaluate the results from these four samples, equation (1) was used to calculate a thermal conductivity-derived particle size for each sample. The results of these extrapolations are summarized in Table 5.

Table 4. Comparison of Thermal Conductivity Measurements[a]

Particle Size, μm		Pressure, torr	Thermal Conductivity, W/m K		Percentage Difference, (A–B)/B
A	B		A	B	
		5	0.10	0.0948	+2.0
650–900	710–900	5	0.10		+2.0
		10	0.12	0.118	+1.7
		5	0.028	0.029	−2.4
40–70	70–75	5	0.034		+17
		10	0.030	0.0416	−28

[a]A, data from Urquhart and Smrekar (unpublished data, 2000); see *Urquhart and Smrekar* [2000]. B, data from Paper 2.

Table 5. Thermal Conductivities and Extrapolated Particle Sizes for Samples With Particles ≤ 1 Φ (>710–900 μm)

	Sample							
	A-3		A-5		A-6		CD-01	
Pressure, torr	Thermal Conductivity, W/m K	Extrapolated Particle Size,[a] μm	Thermal Conductivity, W/m K	Extrapolated Particle Size,[a] μm	Thermal Conductivity, W/m K	Extrapolated Particle Size,[a] μm	Thermal Conductivity, W/m K	Extrapolated Particle Size,[a] μm
3	0.0868	1067	0.104	1547	0.125	2274	0.0950	1284
4	0.105	1357	0.125	1960	0.156	3129	0.0979	1170
5	0.115	1460	0.138	2164	0.170	3396	0.105	1199
6	0.122	1503	0.142	2098	0.184	3712	0.113	1270
8	0.154	2165	0.179	3045	0.206	4189	0.133	1552
Average particle size,[b] μm		1500		2200		3300		1300

[a]Particle sizes are extrapolated from equation (1).
[b]Average particle size rounded off to the nearest 100 μm.

[29] Table 6 is a summary of the results obtained from Figure 4 together with the data in Tables 3 and 5. In 9 of the 11 samples, the thermal conductivity-derived particle size is larger than the median or mean particle sizes of the sample, but smaller than the absolute largest size present. In two samples the derived particle size is essentially equal to the median and mean particle size values. One of these samples, CD-04, has a derived particle size of 3 Φ, but it is especially well sorted, and only ~1 wt.% of the sample is contained in the next larger particle size bin of 2 Φ. The other sample, Sample 1, has a derived particle size of 4 Φ, with only 12.7 wt.% of the particles larger than that size bin.

[30] Included in Table 6 is the weight percent of each sample that is less than or equal to the thermal conductivity-derived particle size, and the weight percent of each sample that is merely less than the thermal conductivity-derived particle size. The value less than or equal to the derived particle size is at least 85 wt.% in all samples and greater than 95 wt.% in all but two samples. Even when the "or equal to" Φ bin is not considered, the thermal conductivity-derived particle size is still greater than 85 wt.% in all but three samples.

[31] Figure 4 illustrates another interesting exception to this result, as seen in Samples 2, 3, 7, and in CD-01 (Figures 4b, 4c, 4g, and 4j). Under atmospheric pressures less than 2 torr, the thermal conductivities of these samples are significantly lower than those of the glass beads that match the larger particle sizes; whereas, above 3 torr, the thermal conductivities are consistent with those of the larger particle sizes. From Table 3 and Figure 3, the samples in question are either fine-skewed or have a relatively high content of finer particles (<250 μm) compared to the other moderately sorted, coarse-skewed samples. While atmospheric pressures on Mars are generally higher than 3 torr, these pressures would be expected at elevations higher than 7.6 km. Nevertheless, even at these low pressures, the data still match well with the thermal conductivities of glass beads in the next largest particle size. In each case, at least 90 wt.% of the sample is still smaller than the thermal conductivity-derived particle size from either pressure range (Figure 3 and Table 6).

6. Discussion

[32] Since equation (1) was used to compute the thermal conductivity-derived particle size of four of the eleven samples, whether it can be used reliably for particle sizes that are larger than those measured in the laboratory must first be assessed. *Jakosky* [1986] notes that thermal conductivity values for particulate materials level off as the atmospheric pressure increases [*Wechsler et al.*, 1972]. Since the actual pore size does not change with atmospheric pressure, this relationship suggests that as the mean free path of the atmospheric molecules decreases with respect to the pore size, the thermal conductivity should reach a near constant value. Extrapolating to Mars atmospheric pressures and temperatures, *Jakosky* [1986] estimates that the thermal conductivity should begin to reach a near constant value for particles larger than about 1 mm. If *Jakosky* [1986] is correct, then equation (1) should not hold for particles larger than this.

[33] Figures 4c, 4e, 4f, and 4k, however, illustrate that the thermal conductivities of Samples 3, 5, 6, and CD-01 all have thermal conductivities that are noticeably higher than those measured for 710–900 μm glass beads. Moreover, Figure 4f illustrates that the thermal conductivities of Sample 6 are significantly higher than those of Sample 5, and Figure 4c illustrates that the thermal conductivities of Sample 5 generally are noticeably higher than those of Sample 3. Figure 6b shows portions of Samples 3, 5, and 6 on a 1 mm grid. Visually, the particle sizes of these samples can be seen to support the relative relationships indicated by their thermal conductivities. Furthermore, the larger particles visible for each sample in Figures 6a and 6b do appear to be in agreement with the average extrapolated particle size calculated from equation (1) (Table 5).

[34] This apparent agreement, however, does not negate the arguments of *Jakosky* [1986]. *Schotte* [1960] points out that most of the thermal transfer occurs near the particle-particle contact points, where particle separation is much smaller than the pore size. Therefore even particles that are more than 1000 times larger than the mean free path will show some dependence of their thermal conductivities on particle size [*Jakosky*, 1986]. The leveling off of thermal conductivity to a near constant value is likely therefore not to be an abrupt occurrence. Moreover, a careful examination of the data in Table 5 shows that the estimated particle size generally increases with increasing atmospheric pressure. If equation (1) truly applied over this range of particle sizes, the calculated values should not show any dependence with atmospheric pressure. This trend suggests that a limit of 1 mm for the applicability of equation (1) may be a valid

Table 6. Statistical Parameters of the Particle Size Distribution of the Samples

Sample	Median Particle Size (Φ)	Mean Particle Size (Φ)	Largest Particle Size (Φ)	Thermal Conductivity-Derived Particle Size			
				Φ	μm	wt.% ≤ Derived Particle Size	wt.% < Derived Particle Size
A-1	4.18	4.01	1	4	70–75	87.3	60.0
A-2	2.89	2.94	0	2	250–275	99.8	99.3
A-3	1.50	1.42	−1	0	1500[a]	98.0	90.3
A-4	2.45	2.44	1	1	500–520	100	99.9
A-5	0.88	0.82	−2	−1	2200[a]	99.5	96.6
A-6	0.68	0.63	−2	−2	3300[a]	100	99.6
A-7	2.72	2.83	0	1	500–520	99.9	99.3
A-8	3.60	3.55	0	2	250–275	99.0	92.8
JSC Mars-1	2.19	2.22	0	1	500–520	99.6	86.9
CD-01	0.10	0.33	−2	0	1300[a]	86.9	52.05
CD-04	2.75	2.75	2	3	160–180	98.8	21.45

[a]Values extrapolated from equation (1). See Table 5.

one. Nonetheless, the arguments in the preceding paragraph suggest that this deviation is not yet severe for particle sizes up to about 3 mm in size and that equation (1) may be appropriately used in such cases, with caution.

[35] Furthermore, *Jakosky* [1986] states that his analysis applies to non-bonded particles of uniform particle sizes and that different pore geometries, adsorption history, or a mixture of particle sizes may produce larger thermal conductivities. However, *Jakosky* [1986] suggests that in a mixture of particle sizes the smaller particles would fill the pores between larger ones, thus raising the conductivity. This interpretation infers that an abundance of smaller particles may be at least as important in controlling the thermal conductivity as the larger particle sizes.

[36] However, while smaller particles will reduce the size of the pore space, they also have a greater number of particle-particle contacts per volume than do larger particles. The capacitor-like effect of these contacts appear to have a greater control over the thermal conductivity than the reduction in pore size as seen by the lower thermal conductivity of smaller particles by themselves compared to that of larger particles [*Wechsler et al.*, 1972; Paper 2].

[37] While the data in this study are not sufficient to examine all competing effects on the bulk thermal conductivity, there is enough information to suggest that in loose sediments, with an intimate mixing of the various particle sizes, an enhancement of thermal conductivity due to small particles filling in the pores between larger particles is not likely to be the primary cause of the observed thermal conductivities. Figure 4, together with the data in Tables 3 and 5, does not illustrate any instance where the thermal conductivity is enhanced over that of the largest particle size. *Woodside and Messmer* [1961] present the only case to date that does show such an enhancement. In their experiment, their mixture is bimodal and the smaller particles are described as completely filling the pore spaces of the larger particles. This description infers that the packing density of the smaller particles within the mixture may have a higher bulk density relative to that of either sample alone. An increase in the bulk density has been shown to increase the thermal conductivity [*Fountain and West*, 1970; *Presley and Christensen*, 1997c, 2006]. Unfortunately, *Woodside and Messmer* [1961] do not report the bulk densities for their samples, so the cause of the enhanced thermal conductivities remains speculative.

[38] Moreover, as pointed out in section 5, samples that are either fine-skewed or that contain a large amount of particles $\leq$250 μm tend to exhibit suppressed thermal conductivities, specifically at low atmospheric pressures, rather than enhanced thermal conductivities. These results are consistent with the lower thermal conductivities exhibited by smaller particle sizes.

[39] The data presented in this study illustrate that virtually the entire sample is composed of particles that are equal to or smaller than the particle size suggested by measurements of the thermal conductivity. The implication is that most of the particles may actually be much smaller than thermal-inertia derived particle sizes for the Martian surface. This result is significant. Currently, the particle size determined from thermal inertia measurements is interpreted as an ''average'' or ''modal'' particle size. These results instead indicate that the thermal inertia-derived particle size is actually closer to a maximum, and that typically at least 85% of the particles are likely to be smaller than the derived particle size.

[40] The significance of this result is that it may allow scientists to distinguish geomorphologic processes acting on the Martian surface. For instance, sediments formed in an eolian environment tend to be much better sorted, and the size of particles present in dunes is limited by the saltation threshold [*Iversen and White*, 1982; *Edgett and Christensen*, 1991]. In contrast, sediments carried and deposited in high-energy fluvial environments tend to be more poorly sorted, and are likely to contain significantly larger particles. These results along with the improving resolution of thermal infrared data suggest that identification of coarser-grained fluvial deposits on the Martian surface may be feasible. Are the dunes visible in so many of the fluvial channels today derived from a simple eolian reworking of the original fluvial deposits, or are they an eolian overprint of material with a different origin? The results presented in this paper may help answer this question.

7. Conclusion

[41] Thermal conductivities were measured for eight natural particle size mixtures and one sample of simulated

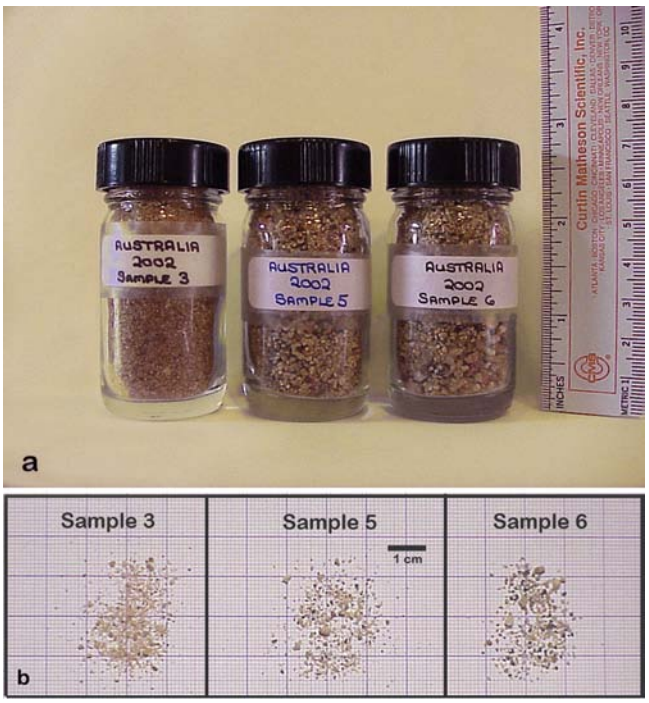

Figure 6. Australia samples 3, 5, and 6. This figure illustrates the progressive increase of particle size with each sample. Extrapolation of previous thermal conductivity-particle size data (Paper 2) appears to describe sufficiently the particle size of these samples. (a) The samples as stored after thermal conductivity measurements. (b) Portions of each sample displayed on a 1 mm grid.

Martian sediment. The particle size distribution was also determined for each of these samples. The measured thermal conductivities were compared to those previously evaluated for narrow particle size ranges (Paper 2), to determine a "thermal conductivity-derived" particle size. Comparison of these derived particle sizes with the actual particle size distributions of the samples indicates that the thermal conductivity, and hence the thermal inertia, reflects the larger particles such that at least 85–95% of the particles are likely to be smaller than or equal to the derived particle size. A thermal inertia-derived particle size therefore is actually closer to a maximum particle size, rather than an average or modal particle size.

[42] **Acknowledgments.** Thorough reviews from Nathan Putzig and Mary Urquhart, together with additional comments from Bruce Jakosky and suggestions from Robin Fergason, significantly improved this manuscript. We are grateful to Sylvain Piqueux for additional discussion; to Evert Fruitman and Bill Coleman for upgrades and repairs to the signal conditioner; to Chris Skiba for supplying the second vacuum pump; to Rossman Irwin, Ruslan Kusmin, and Ted Maxwell for their help collecting the Australian samples in the field; to Alan Levine for the samples of basaltic dune sand; to William Marra for the Mars-1 simulant; to Bryan MacFarlane and Jeff Geier for some of the particle size analysis; and particularly to Phil Christensen for his continuing and unwavering support through a very severe illness (M. Presley's). This study was supported by NASA grants NAG5-12180 and NAG5-10214. The complete data set is stored on a Macintosh Zip disk in the possession of the primary author. Abbreviated data files are kept in hard copy and will be added to the library in the Mars Space Flight Facility at Arizona State University, Tempe, AZ. Data are available upon request from the primary author.

References

Allen, C. C., R. V. Morris, K. M. Jager, D. C. Golden, D. J. Lindstrom, M. M. Lindstrom, and J. P. Lockwood (1998), Martian regolith simulant JSC Mars-1, *Lunar Planet. Sci.*, *XXIX*, abstract 1690.

Carr, M. H. (1981), *The Surface of Mars*, 232 pp., Yale Univ. Press, New Haven, Conn.

Carslaw, H. S., and J. C. Jaeger (1959), *Conduction of Heat in Solids*, 2nd ed., Clarendon, Oxford, U. K.

Christensen, P. R., and M. C. Malin (1988), High resolution thermal imaging of Mars, *XIX Lunar Planet. Sci.*, 180–181.

Christensen, P. R., and H. J. Moore (1992), The Martian surface layer, in *Mars*, edited by H. H. Kieffer et al., pp. 686–729, Univ. of Ariz. Press, Tucson.

Craddock, R. A., and M. A. Presley (2003), Thermal conductivity studies of sedimentary materials from central Australia and the implications for Mars, *Lunar Planet. Sci.*, *XXXIV*, abstract 1612.

Cremers, C. J. (1971), A thermal conductivity cell for small powdered samples, *Rev. Sci. Instrum.*, *42*(11), 1694–1696.

Deissler, R. G., and J. S. Boegli (1958), An investigation of effective thermal conductivities of powders in various gases, *Trans. ASME*, *80*, 1417–1425.

Edgett, K. S., and P. R. Christensen (1991), The particle size of Martian aeolian dunes, *J. Geophys. Res.*, *96*(E5), 22,765–22,776.

Fergason, R. L., and P. R. Christensen (2003), Thermal inertia using THEMIS infrared data, *Lunar Planet. Sci.*, *XXXIV*, abstract 1785.

Fergason, R. L., P. R. Christensen, J. F. Bell III, M. P. Golombek, K. E. Herkenhoff, and H. H. Kieffer (2006a), Physical properties of the Mars Exploration Rover landing sites as inferred from Mini-TES–derived thermal inertia, *J. Geophys. Res.*, *111*, E02S21, doi:10.1029/2005JE002583.

Fergason, R. L., P. R. Christensen, and H. H. Kieffer (2006b), High resolution thermal inertia derived from THEMIS: Thermal model and applications, *J. Geophys. Res.*, doi:10.1029/2006JE002735, in press.

Fountain, J. A., and E. A. West (1970), Thermal conductivity of particulate basalt as a function of density in simulated lunar and Martian environments, *J. Geophys. Res.*, *75*(20), 4063–4069.

Haberle, R. M., and B. M. Jakosky (1991), Atmospheric effects on the remote determination of thermal inertia on Mars, *Icarus*, *90*, 187–204.

Iversen, J. D., and B. R. White (1982), Saltation threshold on Earth, Mars and Venus, *Sedimentology*, *29*, 111–119.

Jakosky, B. M. (1986), On the thermal properties of Martian fines, *Icarus*, *66*, 117–124.

Jones, B. W. (1988), Thermal conductivity probe: Development of method and application to a coarse granular medium, *J. Phys. E Sci. Instrum.*, *21*, 832–839.

Kennard, E. H. (1938), *Kinetic Theory of Gases: With an Introduction to Statistical Mechanics*, 483 pp., McGraw–Hill, New York.

Kieffer, H. H., S. C. Chase Jr., E. Miner, G. Münch, and G. Neugebauer (1973), Preliminary report on infrared radiometric measurements from the Mariner 9 spacecraft, *J. Geophys. Res.*, *78*(20), 4291–4312.

Kieffer, H. H., T. Z. Martin, A. R. Peterfreund, B. M. Jakosky, E. D. Miner, and F. D. Palluconi (1977), Thermal and albedo mapping of Mars during the Viking primary mission, *J. Geophys. Res.*, *82*, 4249–4291.

Kieffer, H. H., P. A. Davis, and L. A. Soderblom (1981), Mars' global properties: Maps and application, *Proc. Lunar Planet. Conf.*, *12B*, 1395–1417.

Kieffer, H. H., B. M. Jakosky, and C. W. Snyder (1992), The planet Mars: From antiquity to the present, in *Mars*, edited by H. H. Kieffer et al., pp. 1–33, Univ. of Ariz. Press, Tucson.

McGee, T. D. (1988), *Principles and Methods of Temperature Measurement*, John Wiley, Hoboken, N. J.

Mellon, M. T., B. M. Jakosky, H. H. Kieffer, and P. R. Christensen (2000), High-resolution thermal inertia mapping from the Mars Global Surveyor Thermal Emission Spectrometer, *Icarus*, *148*, 437–455.

Merényi, E., K. S. Edgett, and R. B. Singer (1996), Deucalionis Regio, Mars: Evidence for a new type of immobile weathered soil unit, *Icarus*, *124*, 296–307.

Moore, W. J. (1972), *Physical Chemistry*, 4th ed., 977 pp., Prentice–Hall, Upper Saddle River, N. J.

Presley, M. A. (1995), Thermal conductivity measurements of particulate materials: Implications for surficial units on Mars, Ph.D. dissertation, Ariz. State Univ., Tempe.

Presley, M. A., and R. E. Arvidson (1988), Nature and origin of materials exposed in the Oxia Palus–Western Arabia–Sinus Meridiani region, Mars, *Icarus*, *75*, 499–517.

Presley, M. A., and P. R. Christensen (1997a), Thermal conductivity measurements of particulate materials: 1. A review, *J. Geophys. Res.*, *102*(E3), 6535–6549.

Presley, M. A., and P. R. Christensen (1997b), Thermal conductivity measurements of particulate materials: 2. Results, *J. Geophys. Res.*, *102*(E3), 6551–6566.

Presley, M. A., and P. R. Christensen (1997c), The effect of bulk density and particle size sorting on the thermal conductivity of particulate materials under Martian atmospheric pressures, *J. Geophys. Res.*, *102*(E4), 9221–9229.

Presley, M. A., and P. R. Christensen (2006), The effect of bulk density on the thermal conductivity of particulate materials under Martian atmospheric pressures, *Lunar Planet. Sci.*, *XXXVII*, abstract 2383.

Putzig, N. E., M. T. Mellon, B. M. Jakosky, S. M. Pelkey, S. Martinez–Alonso, B. M. Hynek, and N. W. Murphy (2004), Mars thermal inertia from THEMIS data, *Lunar Planet. Sci.*, *XXXV*, abstract 1683.

Putzig, N. E., M. T. Mellon, K. A. Kretke, and R. E. Arvidson (2005), Global thermal inertia and surface properties of Mars from the MGS mapping mission, *Icarus*, *173*, 325–341.

Schotte, W. (1960), Thermal conductivity of packed beds, *AIChE J.*, *16*(1), 63–67.

Smoluchowski, M. M. (1910), Sur la conductibilite calorifique des corps pulverizes, *Bull. Int. Acad. Sci. Cacovie*, *5A*, 129–153.

Smrekar, S., et al. (1999), Deep Space 2: The Mars Microprobe Mission, *J. Geophys. Res.*, *104*(E11)), 27,013–27,030.

Stalhane, B., and S. Pyk (1931), New method for determining the coefficients of thermal conductivity, *Tek. Tidskr.*, *61*(28), 389–393.

Urquhart, M. L., and S. E. Smrekar (2000), Estimation of soil thermal conductivity from a Mars Microprobe-type penetrator, *Lunar Planet. Sci.*, *XXXI*, abstract 1781.

Watson, K. I. (1964), The thermal conductivity measurements of selected silicate powders in vacuum from 150–350°K, II, An interpretation of the moon's eclipse and lunation cooling as observed through the Earth's atmosphere from 8–14 microns, Ph.D. dissertation, Calif. Inst. of Technol., Pasadena.

Wechsler, A. E., and P. E. Glaser (1965), Pressure effects on postulated lunar materials, *Icarus*, *4*, 335–352.

Wechsler, A. E., P. E. Glaser, and J. A. Fountain (1972), Thermal properties of granulated materials, in *Thermal Characteristics of the Moon*, edited by J. W. Lucas, *Prog. Astronaut. Aeronaut.*, *28*, 215–241.

Woodside, W., and J. H. Messmer (1961), Thermal conductivity of porous media, I, Unconsolidated sands, *J. Appl. Phys.*, *32*(9), 1688–1699.

R. A. Craddock, Center for Earth and Planetary Studies, National Air and Space Museum, Smithsonian Institution, Washington, DC 20560-0315, USA.

M. A. Presley, School of Earth and Space Exploration, Mars Space Flight Facility, Arizona State University, Box 876305, Tempe, AZ 85287-6305, USA. (mpresley@asu.edu)